CHARACTERISATION AND MODELLING OF THE PLASTIC MATERIAL BEHAVIOUR AND ITS APPLICATION IN SHEET METAL FORMING SIMULATION

Henk Vegter[*], Carel H.L.J. ten Horn[*], Yuguo An[*], Eisso H. Atzema[*], Hermen H. Pijlman[†], Ton H. van den Boogaard[†] and Han Huétink[†]

[*] Corus Research Development & Technology, PO Box 10000, 1970 CA IJmuiden, the Netherlands,
e-mail: henk.vegter@corusgroup.com

[†]University of Twente, PO Box 217, 7500 AE Enschede, the Netherlands,
email: j.huetink@wb.utwente.nl

Key words: Yield Locus, Strain hardening, Sheet metal forming.

Abstract. *The application of simulation models in sheet metal forming in automotive industry has proven to be beneficial to reduce tool costs in the designing stage and for optimising current processes. Moreover, it is a promising tool for a material supplier to optimise material choice and development for both its final application and its forming capacity. The present practice requires a high predictive value of these simulations. The material models in these simulation models need to be developed sufficiently to meet the requirement of the predictions. For the determination of parameters for the material models, mechanical tests at different strain paths are necessary [1]. Usually, the material models implemented in the simulation models are not able to describe the plastic material behaviour during monotonic strain paths sufficiently accurate [2]. This is true for the strain hardening model, the influence of strain rate and the description of the yield locus in these models. A first stage is to implement the improved material models which describe this single strain path behaviour in a better way. In this work, different yield criteria, a hardening model and their comparison to experiments are described extensively. The improved material model has been validated initially on forming limit curves which are determined experimentally with Nakazima strips. These results will be compared with predictions using Marciniak-Kuczinsky-analysis with both the new material model and the conventional material model. Finally, the validation on real pressed products will be shown by comparing simulation results using different material models with the experimental data. The next challenge is the description of the material after a change of strain path. Experimental evidence given here shows that this behaviour cannot be treated using the classical approach of an equivalent strain as the only history variable.*

Henk Vegter, Carel H.L.J. ten Horn, Yuguo An, Eisso H. Atzema,
Hermen H. Pijlman, Ton H. van den Boogaard and Han Huétink

1 INTRODUCTION

The application of simulation models in sheet metal forming in automotive industry has proven to be beneficial to reduce tool costs in the designing stage and for optimising current processes. Also, due to environmental, economic and safety concerns, the car manufacturers need to design lighter and safer vehicles in ever shorter development times. This means that the components have to be designed more critically regarding their forming and crash behaviour. This in turn means that the material models used in forming and crash simulations need to have a higher accuracy. In order to obtain a higher accuracy, the material models need to be improved as well as the mechanical tests that are used to characterise the mechanical behaviour of materials.

The results from the mechanical tests are necessary to determine the parameters of the material models [1,2]. In this work, the mechanical tests will be described as well as several material models and their validation using forming limit curves and real pressed parts.

2 MECHANICAL TESTS TO DETERMINE THE PLASTIC BEHAVIOUR

The basis of the mechanical tests considered are the determination of stress - strain curves under the four key conditions given in figure 1. These four key conditions are: uniaxial tension, plane strain tension, equi-biaxial tension and pure shear. The test procedure presented here allows all four key points to be measured using an ordinary tensile test machine.

Proportional strain paths and loading conditions are used for the derivation of the constants of the material model (i.e. yield locus and hardening behaviour). Later on, also changes of strain path are considered by combining the strain paths of the conditions of figure 1.
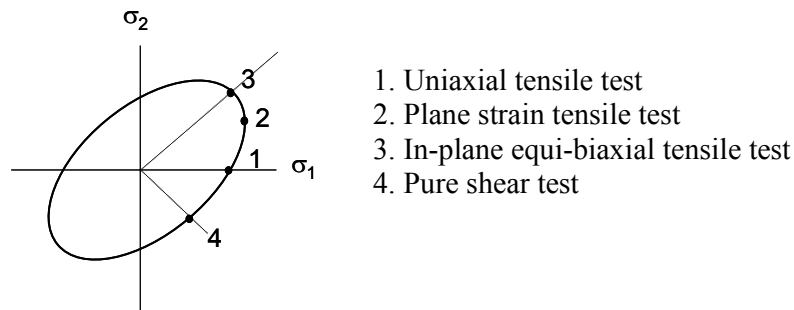

1. Uniaxial tensile test
2. Plane strain tensile test
3. In-plane equi-biaxial tensile test
4. Pure shear test

Figure 1: Four basic mechanical tests

2.1 Tensile tests

The most common mechanical test is the uniaxial tensile test. An advantage is the uniform strain distribution resulting in the high accuracy of the measurements in comparison with other tests to be discussed later. A disadvantage is the relatively small maximum attainable uniform strain due to the plastic instability. As strain rate sensitivity is important for steel, tests are carried out at different strain rates. One of the disturbing effects of testing at non-quasi-static strain rates is heating of the specimen due to the plastic work [1,3]. For LC-steels,

the temperature can be shown to increase by 1°C at every 1% deformation assuming adiabatic heating. In a tensile test this heating results in a temperature increase of about 20 K at the end of uniform straining. The decrease of the yield stress per unit of temperature is approximately 0.5 MPa/K. Therefore the yield stress is approximately 10 MPa lower at the end of uniform straining compared to a completely isothermal tensile test. This means that the temperature effect has a significant influence on the strain hardening and that it cannot be neglected. Figure 2 shows the influence of the temperature rise due to adiabatic heating compared to an isothermal test. Because of the simple geometry of the tensile test specimens, a correction is easily made with a simple temperature model [1,3]. The main processes taken into account are heating in the deformation zone of the specimen and cooling due to conduction of heat to where the specimen is clamped. Depending on the strain rate, the temperature change of the specimen during the test can be anywhere between an isothermal and an adiabatic test. The results of the simple model are compared to measured temperatures in figure 3 for different strain rates. It is clear that even this simple model can estimate the temperature change quite well.
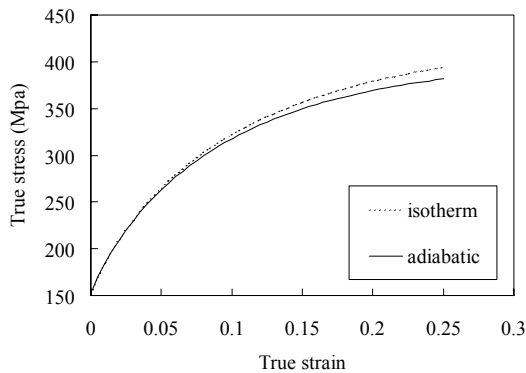

Figure 2: Difference between an adiabatic and isothermal tensile test for an IF-steel at 6.10^{-3} s^{-1} and 22°C
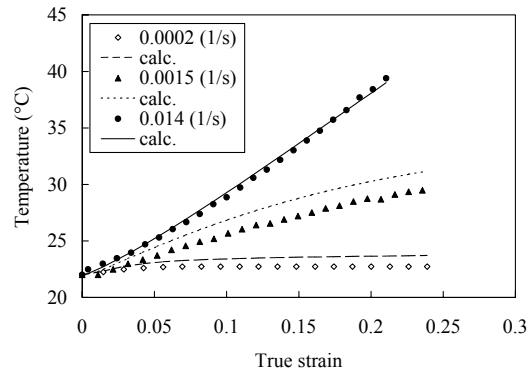
Figure 3: Measured and calculated average temperature as a function of strain at various strain rates.

2.2 Plane strain tensile tests

For the plane strain test, a special specimen has been developed to measure the plane strain stress as a function of strain, see figure 4 [1,3]. The advantage of this specimen is that a plane strain test can be performed using an ordinary tensile testing machine.

One of the difficulties is to achieve a uniform plane strain state over the specimen as is shown in figure 5. Due to the existence of a uniaxial stress state at the edges of the specimen, deviations from a plane strain state always occur in this type of specimen. A correction has to be made to subtract this edge effect from the test results.

A simple geometric average stress – strain curve over the whole width of the specimen would result in a 2% lower value of the plane strain stress. Even such a small difference will

lead to significant differences in the prediction of FLCs and the prediction of strain distribution of critical sheet formed products [2,4].
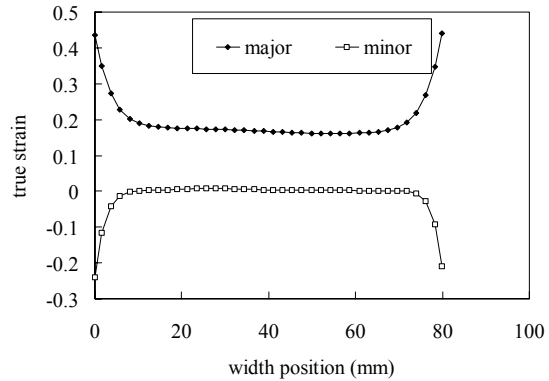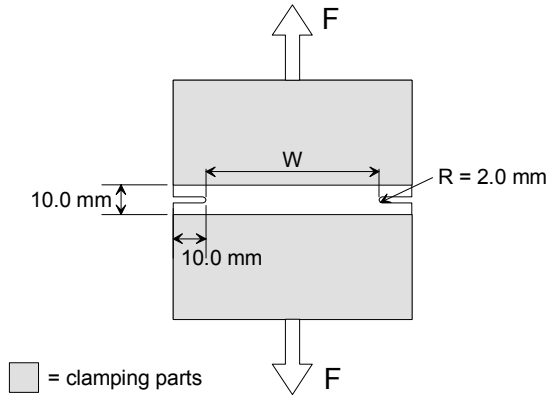

Figure 4: Specimen for the plane strain tensile test at varying width (W = 35 – 81 mm)

Figure 5: Strain distribution of the axial and transverse strain in the plane strain test (LC-steel), W = 81 mm

The new correction procedure has been developed using specimens of different width combined with a measurement of axial strain directly on the mid part of each specimen. In the first draft, the edge effect has been eliminated by relating force - strain curves determined on specimens of different width, see figure 6. In this way, time consuming strain analysis over the width of the specimen including modelling of the test are not necessary anymore. This requires an accurate way of testing with special attention to the clamping. Moreover, these analyses demands a very high accuracy and low amount of spread of these tests at varying width. After analysing examples for some cases, it was not necessary to perform these tests at varying width. For this reason it is proposed to perform the tests at a width of 60 mm.
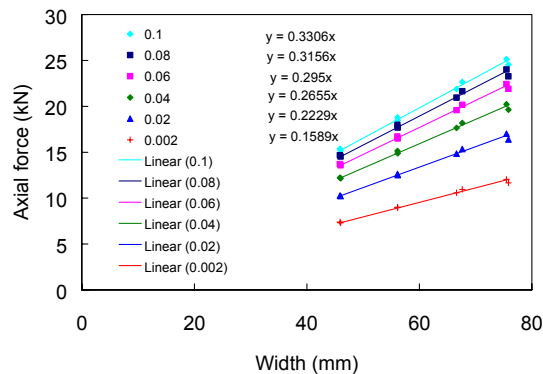
$$F_t = \sigma_{ps} \cdot t \cdot W_c + 2 \cdot F_e$$

Figure 6: Force-width-curves at a certain measured mid-strain. From the slope of the curves the plane strain stress can be derived. (here the edge effect could be neglected; W=W$_c$; F$_e$ =0)

Contrary to the tensile test, temperature effects in the plane strain test do not affect the results significantly due to the small length of the deformation zone of the specimen. This means that the plane strain test is nearly isothermal.

2.3 Equi-biaxial tensile tests

In order to perform tests in the equi-biaxial stress state in a simple way, the in-plane equi-biaxial stress state can be related to compression tests on the sheet plane.

A compression test has been developed using a specimen consisting of stacked square sheets [5]. By applying the load on the sheet plane (see figure 7), the compressive stress can be determined as a function of strain. This compressive stress can be used directly for the equi-biaxial point of the yield criterion. Among the advantages of this method is that an ordinary tensile test machine can be used and that the load and strain can be measured accurately. Also the compression test allows measurement of the stress - strain curve up to high strain levels. In alternative tests such as hydraulic bulging the accuracy is limited due to problems in the determination of the curvature of the specimen.
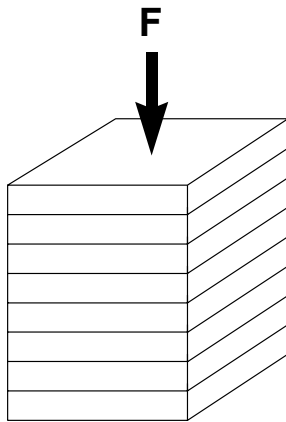

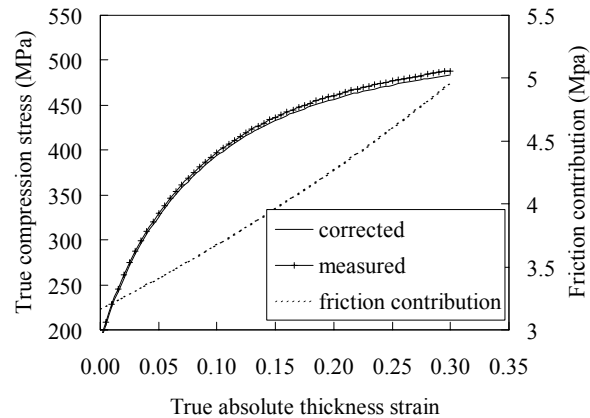Figure 7: Stacked sheet specimen for the compression test

Figure 8: Correction for friction in the compression test for LC-steel

One of the problems to overcome in the compression test is the effect of friction on the sheet plane. Friction has to be suppressed as much as possible. A PTFE-layer combined with a preserving oil has been used as a lubricant. To show the effect of friction the height - diameter ratio of the specimen has been varied. In this case the shear stress for shear deformation of the PTFE-layer determines the friction force along the surface. In figure 8, the friction correction is demonstrated for a compression test stress - strain curve for low carbons steel [6].

2.4 Pure shear test

The fourth mechanical test to be performed is the sheet shear test, see figure 9. The shape

of the test specimen was originally proposed by Miyauchi [7] and later on developed by the University of Twente [8]. This test is particularly important for the description of the plastic material behaviour in the flange part during a deep drawing process. The results given in figure 10 were obtained by analysing grid-lines for individual test specimens by hand; the angle of the vertical grid lines with the original horizontal co-ordinate has to be measured by hand on the centre line in the deformation zones. The test procedure has to be improved to be useful as a standard test. The main problem to overcome is the measurement of the amount of shear on the centre line.
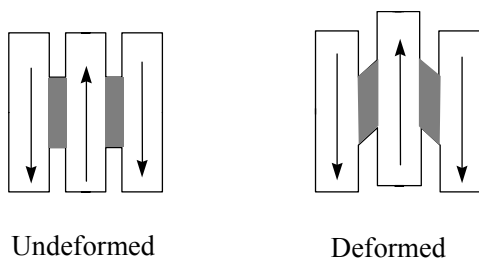

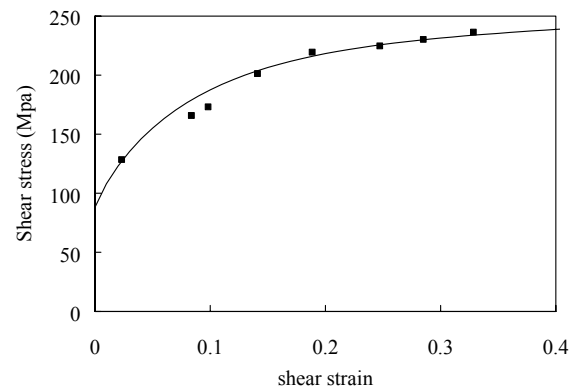Figure 9: Geometry of the pure shear test specimen

Figure 10: Shear stress as a function of shear strain for an IF steel for shear at 45°.

2.5 Multi strain path test

Strain path dependent material behaviour is the next challenge for material models to take into account. Such effects may play an important role during sheet forming processes like stretching and deep drawing in multi stage drawing.

Without presenting theories to describe this type of behaviour some experimental results are shown here. The effect of strain path change from equi-biaxial stretching to uniaxial tension is demonstrated for an IF-steel (figure 11a) and an AA6xxx alloy (figure 11b). The effect on steel is more dramatic because the change of strain path causes an increase of the yield stress followed by a work softening effect. As shown in figure 11 this effect has a large influence on the instability strain in the tensile test. Therefore describing the hardening only with an equivalent plastic strain, as is done in the classical approach, is not sufficient to describe the effect of changes in strain path.

6
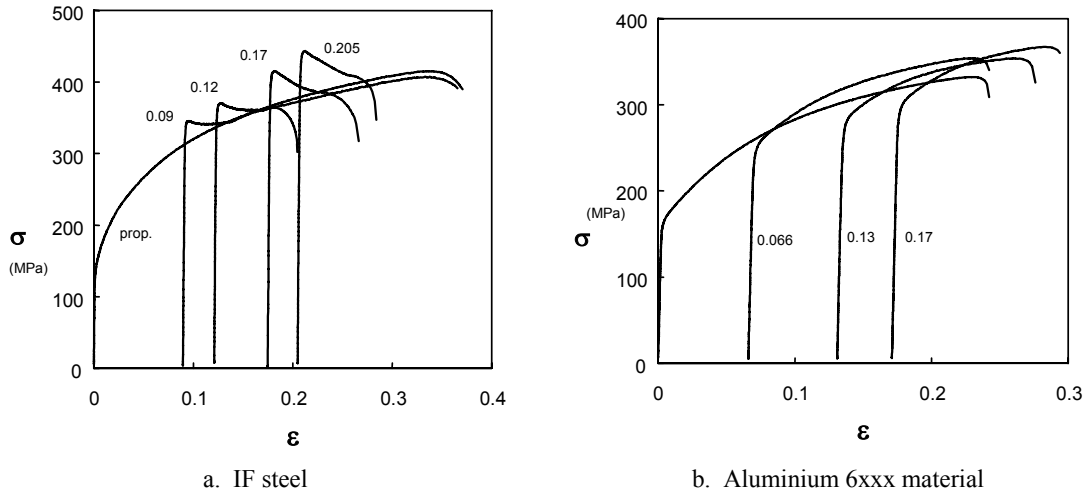
a. IF steel   b. Aluminium 6xxx material

Figure 11: Tensile test curves after various equi-biaxial prestraining; numbers indicate
the thickness strain of the pre-deformation.

3. MATERIAL MODELLING

The data obtained from the tests presented in the previous section, have been used to derive the constants in the material model. The classical approach of a yield criterion combined with a strain hardening model is presented here. This approach can be used also when the influence of the strain path and the change of strain path is included.

3.1 Yield criteria

The plastic flow under multi-axial stress states is described by a yield criterion, which is derived directly from data of tests at the four key stress-states: uniaxial stress, plane strain, equi-biaxial stress and pure shear. For an accurate construction of the yield locus, the stress and strain data in these four key stress-states are necessary.

To find the best yield surface description, several are mutually compared. With each description the number of parameters that need to be determined are stated.

3.1.1 Hill yield criteria

On of the commonly used yield criteria is the Hill-48-criterion which is given in equation 1. For this criterion three parameters have to be determined: R_0, R_{45} and R_{90}.

$$R_0\sigma_y{}^2 + R_{90}\sigma_x{}^2 + R_0R_{90}\left(\sigma_x - \sigma_y\right)^2 + 2\frac{R_0 + R_{90}}{\frac{1}{2} + R_{45}}\tau_{xy}{}^2 = (R_{90} + R_0R_{90})\sigma_{fx}{}^2 \qquad (1)$$

where R_0, R_{45} and R_{90} are the ratio of the transverse to the thickness strain at 0°, 45° and 90° to the rolling direction, respectively. σ_x is the stress in the rolling direction, σ_y is the transverse stress and σ_{fx} is the uniaxial flow stress in the rolling direction.

The Hill-90-criterion [9] is shown in equation 2. It can be considered as an improvement of the Hill-79-criterion. For this criterion 4 parameters have to be determined: α, β, γ and m.

$$
\begin{aligned}
&(\sigma_1 + \sigma_2)^m + \alpha(\sigma_1 - \sigma_2)^m + \\
&(\sigma_1 - \sigma_2)^{\frac{m}{2}-1} \cos(2\phi)\left(\beta\left(\sigma_1{}^2 - \sigma_2{}^2\right) + \gamma(\sigma_1 - \sigma_2)^2 \cos(2\phi)\right) = 2\sigma_f{}^m
\end{aligned}
\tag{2}
$$

where ϕ is the angle between the principal axes of in-plane stress and the principal axes of anisotropy.

The Hill-93-criterion [10] is given in equation 3. A problem regarding this criterion is that it is formulated only for the principal axes of anisotropy (0° en 90° direction). To overcome this, its validity is extrapolated to arbitrary angles to the rolling direction and interpolated with a cosine formulation. In case of a four earing behaviour 7 parameters have to be determined.

$$
\frac{\sigma_1{}^2}{\sigma_{u1}{}^2} + \sigma_1 \cdot \sigma_2 \cdot \left(\frac{1}{\sigma_{u1}{}^2} + \frac{1}{\sigma_{u2}{}^2} - \frac{1}{\sigma_{bi}{}^2}\right) + \frac{\sigma_2{}^2}{\sigma_{u2}{}^2} + \left(p + q - \frac{p \cdot |\sigma_1| + q \cdot |\sigma_2|}{\sigma_{bi}}\right) \cdot \frac{\sigma_1 \cdot \sigma_2}{\sigma_{u1} \cdot \sigma_{u2}} = 1
\tag{3}
$$

where σ_{u1} and σ_{u2} are the uniaxial flow stresses at angle ϕ and $\phi+90^0$ to the rolling direction and σ_{bi} is equi-biaxial flow stress. p and q are constants which have symmetry with each other, i.e. q at angle ϕ is equal to p at angle $\phi+90^0$.

All parameters here depend on the angle ϕ except for σ_{bi}.

3.1.2 Barlat yield criterion

The six component Barlat criterion [11,12,13] is shown in equation 4. In this criterion only three components in the sheet plane are used. It is also suitable to describe the yield function in general three dimensional situations, not just for the plane stress state. In the general case, the criterion requires 9 parameters to be determined: c_1, c_2, c_3, c_4, c_5, c_6, α_x, α_y and m. An arbitrary value for α_z (= 1) has to be chosen. For the plane stress state only 7 parameters need to be determined; parameters c_4 and c_5 are not relevant in this case.

$$
\alpha_1 \cdot |s_2 - s_3|^m + \alpha_2 \cdot |s_3 - s_1|^m + \alpha_3 \cdot |s_1 - s_2|^m = 2 \cdot \sigma_f
$$

$$
\begin{bmatrix} s_x \\ s_y \\ s_z \\ s_{yz} \\ s_{zx} \\ s_{xy} \end{bmatrix} = \begin{bmatrix} (c_2 + c_3)/3 & -c_3/3 & -c_2/3 & 0 & 0 & 0 \\ -c_3/3 & (c_3 + c_1)/3 & -c_1/3 & 0 & 0 & 0 \\ -c_2/3 & -c_1/3 & (c_1 + c_2)/3 & 0 & 0 & 0 \\ 0 & 0 & 0 & c_4 & 0 & 0 \\ 0 & 0 & 0 & 0 & c_5 & 0 \\ 0 & 0 & 0 & 0 & 0 & c_6 \end{bmatrix} \cdot \begin{bmatrix} \sigma_x \\ \sigma_y \\ \sigma_z \\ \sigma_{yz} \\ \sigma_{zx} \\ \sigma_{xy} \end{bmatrix}
\tag{4}
$$

where s_1, s_1 and s_3 are eigenvalues of the s tensor described above (principal axes of s) and α_1, α_2 and α_3 are calculated via transformation to the principal axes of the s-tensor from the

known values of α_x, α_y and α_z for the principal axes of anisotropy.

3.1.3 Vegter yield criterion

The Vegter criterion [1,2,4,14,15,16,8,17,18] is based on Bezier interpolation between reference points in the principal stress space at various angles to the rolling direction, see figure 12. The Bezier interpolation is described in equation 5 for $\overline{\sigma} = \sigma_f$ and an angle ϕ.

$$\begin{pmatrix} \sigma_1 \\ \sigma_2 \end{pmatrix} = (1-\lambda)^2 \cdot \begin{pmatrix} \sigma_1 \\ \sigma_2 \end{pmatrix}_i^r + 2 \cdot \lambda \cdot (1-\lambda) \cdot \begin{pmatrix} \sigma_1 \\ \sigma_2 \end{pmatrix}_i^h + \lambda^2 \cdot \begin{pmatrix} \sigma_1 \\ \sigma_2 \end{pmatrix}_{i+1}^r \tag{5}$$

where ϕ is the angle between the principal axes of plane stress and the principal axes of anisotropy and λ is the parameter for Bezier interpolation. In this equation the superscript r refers to the reference points of the interpolation while superscript h refers to the hinge points.

The hinge points of the interpolation are derived from the strain vector in the two adjacent reference points i and i+1.
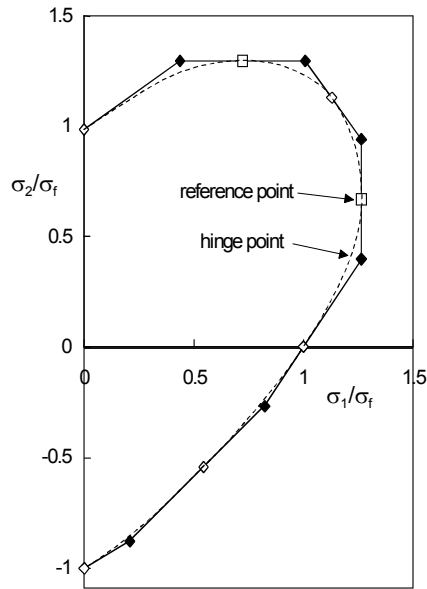

Figure 12: Construction of the yield locus by means of Bezier interpolation in the Vegter yield criterion.

In order to obtain the yield loci at arbitrary angles to the rolling direction, a cosine interpolation of the reference points is used. This is shown in equation 6.

$$\begin{pmatrix} \sigma_1 \\ \sigma_2 \end{pmatrix}_i^r = \sum_{j=0}^{m\cos} \begin{pmatrix} a_1^j \\ a_2^j \end{pmatrix}_i^r \cdot \cos(2 \cdot j \cdot \phi) \tag{6}$$

where mcos is the number of cosine terms used for the expansion of the reference points

and $\begin{pmatrix} a_1{}^j \\ a_2{}^j \end{pmatrix}_i^r$ are parameters for the cosine interpolation to be determined for the reference points.

The cosine interpolation of the R-values is given by equation 7.

$$R(\varphi) = \sum_{j=0}^{m\,cos} b^j \cdot \cos(2 \cdot j \cdot \phi) \tag{7}$$

where b^j are parameters for the cosine interpolation of the R-values.

The Vegter yield criterion needs three data for each reference point: both in-plane stress components and the strain vector, ρ ($= \delta\varepsilon_2/\delta\varepsilon_1$). The reference points are chosen to coincide with the tests performed in the four key stress states.

Due to the choice of fixed stress states or strain states in the reference points, two or fewer unknowns have to be determined in these points:

- pure shear: $\rho = -1$, the pure shear stresses are needed; for this point symmetry exists for the angles ϕ and $\phi+90°$. This point could also be defined from the view point of the stress ($\sigma_2=-\sigma_1$), then the strain vector has to be determined.
- uniaxial tension: $\sigma_2 = 0$, the uniaxial stress and the R-value are needed; the latter provides the strain vector.
- plane strain: $\rho = 0$, the two plane strain stress components are both necessary.
- equi-biaxial: $\sigma_2 = \sigma_1$, the equi-biaxial stress and the strain vector are needed which are valid for every direction.

In case of a four earing anisotropy this criterion needs 17 parameters to be determined. The formulation can be easily extended by using more reference points and more angles with respect to the rolling direction.

The Vegter criterion is the most suitable to fit all the data in the plane stress situation. This criterion needs more parameters to be determined (17 in total) than the quantities which are measured (14) in case of a four fold anisotropy. Therefore some freedom still exists for the plane strain point; the second component can be chosen between the neighbouring two hinge points [4]. In most cases a mid-position between the uniaxial and equi-biaxial point is used.

Because of the large number of parameters, the flexibility of the Vegter criterion also allows it to be fitted to a yield locus that is calculated from the crystallographic texture of the material. This way a texture based yield locus can be easily implemented in simulations.

3.1.4 Comparison of the criteria

As the number of parameters for the Vegter criterion is larger than the number of measured quantities, it can represent all measured data perfectly. The other criteria have fewer parameters than measured quantities and therefore need a least squares method for determining the parameter. Among these other criteria, the Barlat-criterion is the most suited to accommodate the measured quantities. In figure 13b a small difference is visible when it is compared to the Vegter criterion for IF steels. The Hill-criteria still deviate from the measured data. Notably the major plane strain stress is overestimated, whereas the equi-biaxial stress is underestimated, see figure 13a. The Hill yield loci has a more rounded shape than in case of the Vegter-criterion which reflects the measured data most accurately. The same trends are

found for the low carbon steel group in general (not only IF-steel). The over-estimation of the Hill48 criterion for both the plane strain stress and the equi-biaxial stress with respect to measured data is obvious. This will certainly lead to overestimation of deep draw-ability.
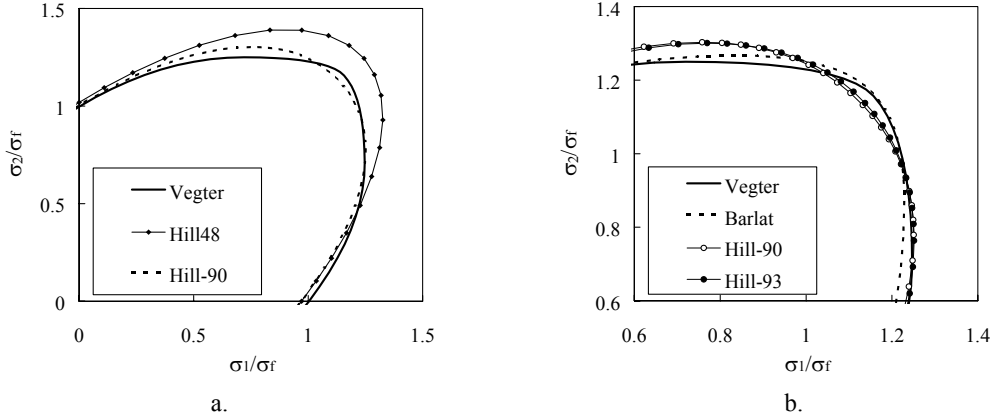

a.   b.

Figure 13: Comparison of different yield locus descriptions at 0^0 to the rolling direction for IF-steel

3.2 The strain hardening relation

Strain hardening is described using an extended Bergström relation [19,20]. To the original Bergström relation, the effect of strain rate and temperature are added as well as an improved behaviour at high levels of strain [21]. This results into the following relationship for the flow stress as a function of strain, strain rate and temperature [3,18,4]:

$$\sigma_f = \sigma_0 + \Delta\sigma_m \cdot \left[\beta \cdot (\overline{\varepsilon} + \varepsilon_0) - e^{-\Omega \cdot (\varepsilon + \varepsilon_0)}\right]^{n'} + \sigma_0^* \cdot \left[1 + \frac{k \cdot T}{\Delta G_0} \cdot \ln\left(\frac{\dot{\varepsilon}}{\dot{\varepsilon}_0}\right)\right]^{m'} \quad (8)$$

σ_0 = static yield stress
$\Delta\sigma_m$ = stress increase parameter for strain hardening
β = strain hardening parameter for large strain behaviour
Ω = strain hardening parameter for small strain behaviour
ε_0 = pre-deformation parameter
n' = exponent for the strain hardening behaviour

σ_0^* = limit dynamic flow stress
ΔG_0 = maximum activation enthalpy,
m' = power for the strain rate behaviour
k = Boltzmann constant = $8.617.10^{-5}$ eV/K
T = absolute temperature in (K)
$\dot{\varepsilon}_0$ = limit strain rate for thermal activated movement

As this equation also contains the temperature, the temperature increase seen in the tensile tests can be accounted for. Instead of providing measured temperature changes to equation 8, values that were calculated using the simple temperature calculation model presented in section 2.1, may also be used.

11

3.3 Strain path dependent material models

In general both the strain hardening relation and the yield criterion can be dependent on the strain path change for different reasons:

- The strain hardening relation is influenced by the way the dislocation network develops with its strain path. Teodosiu [22] presented a model that takes both short term effects after a change and long term effects after a change of strain path into account.
- The yield criterion will change due to the change of crystallographic texture during deformation. This effect reflects a more gradual change [23].

It is obvious that additional strain history parameters have to be used in addition to the equivalent plastic strain to include these type of effects. However, this will not be treated here.

3.4 Parameters of the models for several materials

Using the mechanical tests that were described in the sections 2.1 to 2.4, the points of the yield locus were measured and the results can be seen in table 1. Due to the difficulty in measuring the shear strain for the pure shear point, the values seen in table 1 are estimated values that are derived from the texture based yield criteria. The strain vector for the biaxial point, $(\delta\varepsilon_2/\delta\varepsilon_1)_{bi}$, is determined from the compression tests.

Yield criterion reference stress points and R-value						
Material	R	σ_{un}/σ_f	σ_{sh}/σ_f	σ_{ps}/σ_f	σ_{bi}/σ_f	$(\delta\varepsilon_2/\delta\varepsilon_1)_{bi}$
IF-steel-0°	1.85	1.004	0.538	1.247	1.157	0.777
IF-steel-45°	2.06	0.998	0.544	1.252	1.157	
IF-steel-90°	2.51	0.997	0.538	1.250	1.157	
IF-steel-mean	2.12	1.000	0.541	1.250	1.157	
LC-steel-0°	2.04	0.978	0.524	1.228	1.113	1.02
LC-steel-45°	1.27	1.029	0.565	1.213	1.113	
LC-steel-90°	2.19	0.964	0.524	1.221	1.113	
LC-mean	1.69	1.000	0.544	1.219	1.113	
Al-5xxx-0°	0.73	0.992	0.596	1.081	1.026	1.00
Al-5xxx-45°	0.79	1.008	0.579	1.071	1.026	
Al-5xxx-90°	0.67	0.992	0.556	1.054	1.026	
Al-5xxx-mean	0.75	1.000	0.578	1.069	1.026	

Table 1: Planar anisotropic yield loci constants for three materials based on the uniaxial tensile test, plane strain tensile test and the compression test on the sheet plane.

To describe the hardening behaviour of the material, the extended Bergström model was fitted to the measured data. The obtained parameters for three materials are shown in table 2.

Strain hardening constants						Strain rate constants			
Material	σ_0 (MPa)	$\Delta\sigma_m$ (MPa)	β	Ω	ε_0 fixed	n' fixed	σ^*_0 (MPa) (lit.)	ΔG_0 (eV) (lit.)	m' (lit)	$\dot{\varepsilon}_0$ (s^{-1}) (lit.)
IF-steel	96.2	271.0	0.250	9.27	0.005	0.75	600.0	0.8	2.2	10^8
LC-steel	146.8	218.5	0.462	7.75	0.005	0.75	591.1	0.8	2.2	10^8
Al-5xxx	125.5	261.8	0.100	6.31	0.000	0.75	0.0	0.8	1.0	10^8

Table 2: Constants for the extended Bergström relationship (equation 8) for three materials.

4. FORMING TESTS

4.1 Determination and prediction of the FLD

FLD-tests were carried out by stretching Nakazima strips over a hemispherical punch with a diameter of 75 mm. A special rubber like foil was used as a lubricant on the punch head. The instability strains are derived in failed specimens. In figure 14, the strain distribution and an image is shown of such a specimen under plane strain conditions. The localised necking zone including the crack has to be removed from the more uniformly deforming part of the specimen [24] as shown in figure 15. From the remaining strain distribution the strain limits just before the occurrence of localised necking has to be reconstructed. This has been realised by means of parabolic smoothing on five points at every side of the necking zone. In case of the left hand side (LHS) of the FLD, it was not easy to separate the width necking effect from the more local thickness necking effect. The latter one is more interesting concerning the localised neck, which we intend to determine. Besides the experimental set-up, a source for deviations in limit strains between different FLC-measurement methods is the way of determining the onset of necking from the measured strain distributions. In the IDDRG working-groups and other international forums, this is still under discussion.

Besides the experimental FLC, simulations have been performed to predict the FLC. As an example the FL prediction results is given for IF-steel. The FLD-model is based on the Marciniak - Kuczinsky (MK) theory [25], using an initial thickness defect of 0.01 %. For the LHS of the FLD, the original MK-approach has been changed; the strain state outside was assumed to be proportional to the one inside the groove. For the simulations a two stage deformation process has been chosen. Due to the dome shape of the punch, all specimens were assumed to be biaxially pre-strained up to a level of 0.05 ($\varepsilon_1 = \varepsilon_2 = 0.05$). From this different strain, combinations will occur depending on the width of the specimens. Due to the assumption of proportional hardening, the LHS of the FLD is determined only by the strain hardening and strain rate relation and does not depend on the shape of the yield criterion. For this reason, the thickness defect of 0.01% and the amount of biaxial pre-strain are adjusted for both materials for the LHS. This approach suits both materials. The assumption of an initial thickness defect is a weak point in the MK-theory.

In the FLD-simulation program, only the Vegter criterion was implemented. The results for the other yield criteria were obtained by fitting the Vegter yield locus to the other yield loci. The four different yield loci lead to significantly different results in the prediction of the right

hand side (RHS) of the FLD. Due to the relatively large difference between the major plane strain stress and the equi-biaxial stress in both the Hill-90-criterion and the Hill-93-criterion (figure 13a), the FLD will be over-predicted on the RHS (figure 16). The use of the Barlat-criterion leads to some over-prediction of the FLD for the steel used here and differs significantly from the one predicted with the Vegter yield criterion (figure 16), while the shape between the yield loci is very small (figure 13b). This demonstrates the extreme sensitivity of the FLC prediction to the yield locus shape.
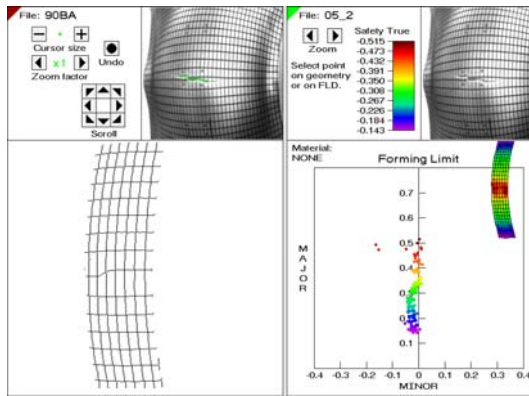

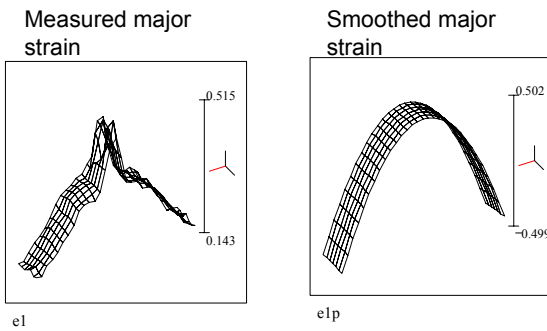Figure 14: FLD measurement Nakazima sample around plane strain

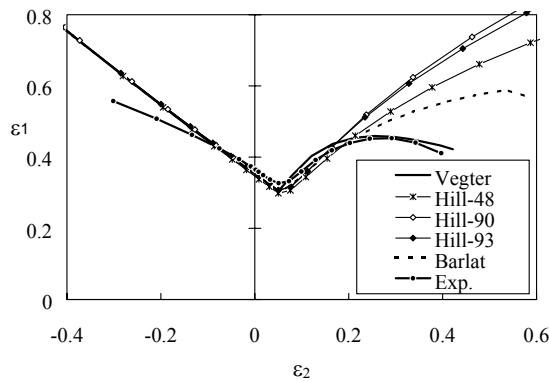Figure 15: Major strain distribution before and after smoothing

Figure 16: FLD-predictions for the IF-steel (90° to RD) using different yield criteria and comparison with experiments

4.2 Stretch forming test on steel

On a low carbon steel, a stretch forming test on a nearly hemispherical punch has been used for validation of the material model in sheet forming simulations. The punch diameter in this case was 75 mm; a standard preserving oil was used as a lubricant; a friction coefficient of a value of 0.16 was measured during friction tests under boundary lubrication conditions [26],

representing the friction condition during punch stretching. Details of the test are given in table 3.

Blank diameter	150 mm
punch diameter	75 mm
die-hole diameter	78.4 mm
punch radius	22.5 mm
die radius	3 mm
friction coefficient	0.16
blank holder force	200 kN

Table 3: Geometry parameters and process parameters for the stretch forming part

In this case an axi-symmetric finite difference model has been used. Such a simulation is justified because the material demonstrates only a small deviation from planar isotropy in the area between the plane strain state and the equi-biaxial stress state (representing the conditions during punch stretching).

The results of the calculated thickness strain for the different yield criteria can be seen in figure 17. In this figure also the experimental results are shown. The Vegter criterion is over the whole blank closest to the experimental data. The other criteria are in order of decreasing accuracy: Barlat, Hill-48, Hill-93 and Hill-90.
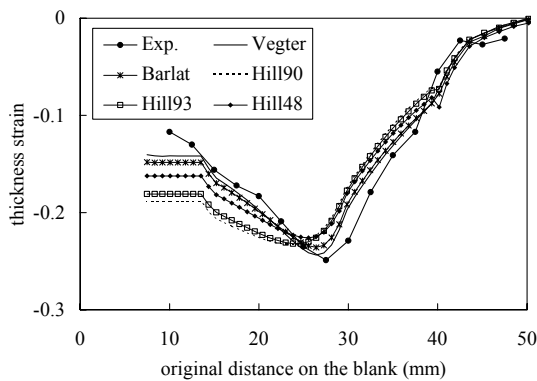

Figure 17: Predicted strain distributions at a product height of 15 mm and comparison with experiments (LC-steel) using different yield locus descriptions.
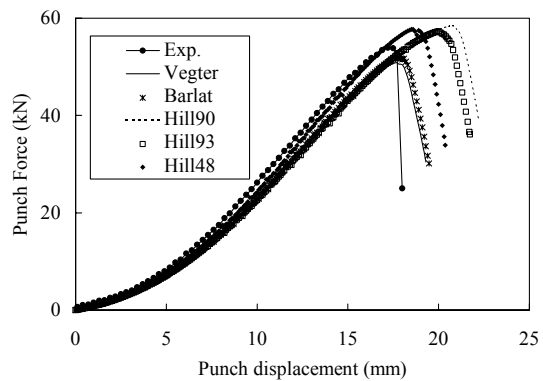
Figure 18: Predicted strain distributions and comparison with experiments (LC-steel) using different yield locus descriptions.

The predicted force displacement curves are given in figure 18. Some small irregularities occur in the force prediction due to the discretisation of the geometry. The punch displacement at the maximum force can be considered to be the point where plastic instability starts. The Vegter yield criterion and the Barlat criterion give nearly the same results. The Hill-48 gives surprisingly good results in comparison with the both improved Hill-90 and

15

Hill-93 criteria. The reason is just good luck for stretch forming simulations in particular. The other two Hill criteria were optimised for all the stress states also for the uniaxial stress state and pure shear state.

4.3 Validation on aluminium test product

In order to validate the Vegter criterion and the extended Bergström model with experimental data for a more complex product, an example is chosen where the forming is critical, i.e. with process conditions such that the product can just be manufactured without failure of the material. For this test a trapezium-shaped product was used. The process parameters can be found in table 4 while the geometry of the drawing die can be seen in figure 19.
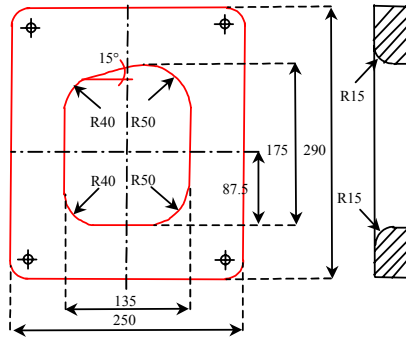

Figure 19. Geometry of the drawing die for the trapezium-shaped product.

blank holder force	5 kN
friction coefficient	0.16
punch displacement	45.5 mm

Table 4. Process parameters for trapezium-shaped product.

The strain distribution in one of the corners of the product was measured experimentally. Alongside these experiments, simulations were performed to obtain the strain distributions when the Hill-48 or Vegter criterion was used. The differences between these two yield criteria can be seen in figure 20. In figure 21, the calculated strain distributions are compared with the experiments. In this figure also the FLC for this material is presented. It can be seen clearly that the Hill-48 criterion predicts that the product is non-critical, while the Vegter criterion and the experiments show that failure occurs during forming.

The Hill criterion shows a strain distribution which tends more to the equi-biaxial state. The different strain distributions can be explained by the yield surface shapes seen in figure 20. The equi-biaxial stress of the Hill criterion is smaller than the value of the Vegter criterion. Therefore the simulation with the Hill criterion will show more deformation at the bottom of the product, where the stress state tends towards equi-biaxial. The Vegter criterion will show more deformation in the wall, where the stress tends to the plane strain state. As a

consequence the Vegter criterion predicts a critical product and the Hill criterion a non-critical product.

It can be concluded that in the trapezium-shaped product the plane strain and equi-biaxial yield stress play an important role in the strain distribution under critical conditions. Because the Vegter yield surface is more accurate in the plane strain and equi-biaxial regions, it provides a better prediction of the strain distribution.
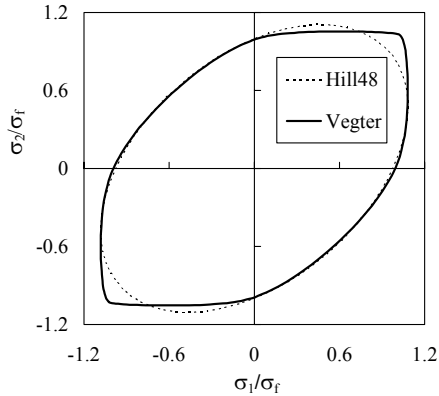

Figure 20: Comparison of the Vegter yield locus with the Hill48 yield locus for AL5XXX alloy
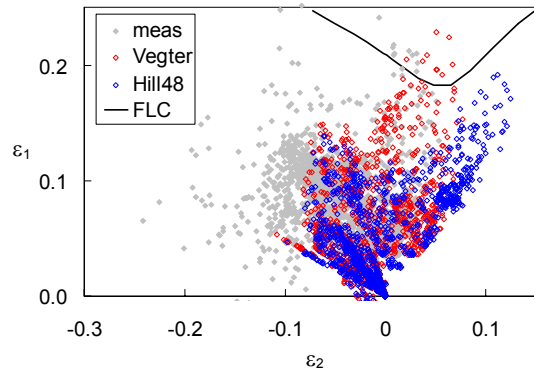
Figure 21: Comparison of simulations using Hill48 yield locus and the Vegter yield criterion

4.4 Real pressed products: Numisheet '99 benchmark

In order to evaluate the Vegter criterion in conjunction with the extended Bergström hardening model for real automotive pressed parts, the benchmark of the Numisheet '99 conference was chosen. This benchmark consisted of the forming process of an Audi front door panel. The simulation was performed with the finite element program DiekA for both the Hill-48-criterion and the Vegter criterion. Unfortunately the results of the simulation can not be interpreted quantitatively as the draw beads were left out. Therefore this simulation should only be considered as an illustration. The computation time needed for the simulation using the Hill-48-criterion was 10 hours and 25 minutes on a HPJ5600 system. When the Vegter-criterion was used the complete simulation only took 8 hours and 53 minutes on the same system. This means that the higher accuracy of the Vegter criterion does not come at the expense of extra computational time. It is therefore fast enough for complete automotive pressings to be evaluated.

5. CONCLUSION

- By the means of mechanical test for four different strain modes, the plastic material behaviour can be derived effectively in such a way that it can be used in material models describing this behaviour.

17

- From the yield criteria considered, the Vegter criterion is most suited to fit all data under plane stress, which is the case for nearly all sheet metal forming processes.
- The Barlat criterion is able to include a real three dimensional stress state and can be seen as a substantial extension of both the Hill-48-criterion and the Hill-79-criterion.
- The Hill-90 and Hill-93 criteria can be considered as a step forward for plane stress use in comparison with the Hill-48-criterion, but do not result in sufficiently accurate predictions in all cases of sheet forming simulations.
- The FLD prediction between plane strain and equi-biaxial stretching is extremely sensitive to the shape of the yield locus. A weak point in the MK theory is the assumption needed regarding to the size of the initial thickness defect.
- The prediction of strain distribution of stretch forming parts of aluminium killed low carbons steels and aluminium 5182 which makes use of the advanced material model are in better agreement with the measured ones. For the steel stretch forming part the onset of necking is predicted in a much better way with this model.
- The new material model does not lead to high CPU-times for complex industrial parts in comparison with the ones making use of the classical theory.

REFERENCES

[1] Vegter H, An Y, Pijlman H.H, Huétink J, *Advanced Mechanical Testing on Aluminium Alloys and Low Carbon Steels for Sheet Forming,* Keynote-lecture, To be published in Proceedings NUMISHEET'99 (Besançon France), J.C. Gelin, et. al. eds, University of Franche Comté (1999)

[2] Vegter H, An Y, Pijlman H.H, Huétink J, *Different Approaches to Describe the Plastic Material Behaviour of Steel and Aluminium-Alloys in Sheet Forming.* Invited paper in proceedings 2nd Esaform , pp127-132 (Guimarães, Portugal), J.A. Covas ed. University of Minho (1999)

[3] Vegter, H., *On the Plastic Behaviour of Steel During Sheet Forming*, Dissertation, University of Twente, The Netherlands, (1991)

[4] Vegter, H., An, Y., Pijlman, H.H., Huétink, J., *Advanced material models in simulation of sheet forming processes and prediction of forming limits*: In proceedings EsaForm 1 (1998), pp. 499-514

[5] An, Y., Vegter, H., *The Difference in Plastic Behaviour between Bulging Test and Through Thickness Compression Test for Sheet Steels and Al-alloys,* IDDRG Working Groups Meeting, 1998 (Genval, Belgium, 1998)

[6] An, Y., Vegter, H., *Experimental study of the friction behavior in the compression test*, IDDRG Working Groups meetings, 1999

[7] Miyauchi, K., *Some interesting behaviour of prestrained sheet metals in press forming*, IDDRG Working Group meetings, 1985

[8] Boogaard, A.H. van den, *Thermally Enhanced Forming of Aluminium Sheet (Modelling and experiments)*, Dissertation, University of Twente, The Netherlands

[9]   Hill, R., *Constitutive Modelling of Orthotropic Plasticity in Sheet Metals,* J. Mech. Phys. Solids, 38 (1990), pp. 405-417.

[10] Hill, R., *A User-Friendly Theory of Orthotropic Plasticity in Sheet Metals,* Int. J. Mech. Sci, 35 (1993), pp. 19-25

[11] Chung, K., Shah, K., *Sheet Forming Simulation Based on Barlat's Planar Anisotropic Yield Criterion,* In proceedings of Mechanical Behaviour of Materials VI, (Kyoto, Japan, 1991), pp. 221-226, eds. M. Jono, T. Inoue, Permagon Press, 1991

[12] Brem, J.C., Barlat, F., Chang, K., *AB2.1 Constitutive Equation Benchmark,* In Proceedings Numisheet' 96 (Dearborn, Michigan. USA, 1996), J.K. Lee, et. al. eds, The Ohio State University (1996), pp. 824-825

[13] Barlat, F., Lege, D.J., Brem, J.C., *A Six Component Yield Function for Anisotropic Materials,* Int. J. of Plast, 7 (1991), pp. 693-712.

[14] Carleer , B.D., *Finite Element Analysis of Deep Drawing*, Dissertation, University of Twente, The Netherlands, (1997)

[15] Pijlman H.H. et al, *The Vegter Yield Criterion on Multi Axial Measurements*, In Proceedings NUMISHEET'99 (Besançon France), J.C. Gelin, et. al. eds, University of Franche Comté

[16] Pijlman H.H (2001), *Sheet Metal Characterization By Bi-axial Experiments* - Dissertation, University of Twente, The Netherlands

[17] Pijlman, H.H., Carleer, B.D., Huétink, J., Vegter, H., *Application of the Vegter Yield Criterion and a Physically Based Hardening Rule on Simulation of Sheet Forming,* In Proceedings of Numiform' 98 (Enschede , the Netherlands,1998), Huétink, J., Baaijens, F.P.T., eds, Balkema/Rotterdam/Brookfield, 1998, pp. 763-768

[18] Vegter, H., Neve, P.F., Langerak, N.A.J., *AB2.2 Constitutive Equation Benchmark,* In Proceedings Numisheet' 96 (Dearborn, Michigan. USA, 1996), J.K. Lee, et. al. eds, The Ohio State University (1996), pp. 826-833

[19] Bergström, Y., *A Dislocation Model for the Stress Strain Behaviour of Polycrystalline α-Fe with Special Emphasis on the Variation of the Densities of Mobile and Immobile Dislocations*, Mat. Sci. Eng. 5, (1969/70.), pp. 179-192

[20] Liempt, P. van, *Workhardening and Substructral Geometry of Metals*, In Proceedings Metal Forming 94, (Birmingham, UK, 1994), P. Hartley, et. al. eds., J. Mat. Proc. Techn, 45 (1994), pp.459-464

[21] Krabiell, A., Dahl, W., *Zum Einfluss von Temperatur und Dehngeschwindigkeit auf die Streckgrenze von Baustahlen unterschiedlicher Festigkeit*, Arch. Eisenhüttenwesen 52, (1982), pp. 429-436

[22] Teodosiu, C., Hu, Z., *Evolution of the intergranular microstructure at moderate and large strains: Modelling and computational significance*, in Simulation of Materials Processing: Theory, Methods and Applications, Shen et.al. eds, Balkema, Rotterdam, 1995

[23] Peeters, B., Seefeldt, M., Teodosiu, C., Kalidindi, S.R., Houtte, P. van, Aernoudt, E., *Work-hardening/softening behaviour of B.C.C. polycrystals during changing strain paths: I*, Acta Materialia vol.49, 2001, p1607-1619

[24] Monfort, G., *BDDRG Working Group Summary of the Experimental FLD-work,*
IDDRG Working Groups Meeting, 1998 (Genval, Belgium, 1998)

[25] Marciniak, Z., Kuczynski, K., *Limit Strains in Processing of Stretch Forming Sheet
Metal*, Int. J. Mech. Sci. 9, (1967), pp. 609-620

[26] Emmens, W.C., *The influence of surface roughness on friction*, 15th biannial IDDRG
congress, Dearborn-Michigan, 1988